

Small- x Behaviour of Lightcone Wavefunctions in Transverse Lattice Gauge Theory

J. Bratt*, S. Dalley†, B. van de Sande*, and E. M. Watson*

**Geneva College*

3200 College Ave.,

Beaver Falls, PA 15010 and

†Department of Physics, University of Wales Swansea

Singleton Park, Swansea SA2 8PP, U.K.

Abstract

We study the behaviour of lightcone wavefunctions, in coarse transverse lattice gauge theory, when one or more parton lightcone momenta are small. This probes the limit of hadron structure at large and small Bjorken x . Finite-energy boundary conditions on boundstates allow one to derive the analytic form of wavefunctions in this region. This leads to simple, universal predictions for the behaviour of quark generalised parton distributions near their endpoints. For the first few meson wavefunctions at large N_c , we give the simplest ansatz that incorporates all the boundary conditions.

1. INTRODUCTION

Transverse lattice gauge theory [1, 2] is a promising approach for ab-initio calculations of the hadronic light-cone wavefunctions. All successful calculations so far have been performed on coarse transverse lattices with effective ‘colour-dielectric’ degrees of freedom, keeping the longitudinal coordinates $x^- = (x^0 - x^3)/\sqrt{2}$ continuous. Although this has required some parameters in the effective Hamiltonian to be fit phenomenologically, it has the great computational advantages that hadrons are dominated by states containing few partons and there is a clean separation between the longitudinal and transverse dynamics. In fact, in this case, it is not much harder to analyse the dependence of wavefunctions on the longitudinal coordinates than in $1+1$ -dimensional gauge theories. While the full wavefunction of a boundstate typically requires—even in $1+1$ dimensions—a numerical solution, the behaviour when parton lightcone momenta k^+ vanish can be largely understood analytically. The prototype example is $1+1$ -dimensional large- N_c QCD [3], where the behaviour of the meson wavefunction for vanishing quark k^+ was found exactly. A similar analysis can be performed to some extent even in $3+1$ -dimensional large- N_c QCD [4]. The key strategy in all cases is to demand cancellation of singularities in the lightcone boundstate Schrodinger equation when parton lightcone momenta vanish. Typically, wavefunctions do not simply vanish in this high free-energy limit, as they would at large transverse momentum. Rather, there occur ‘ladder’ relations between states with different numbers of partons that couple the analytic structure of the infinite tower of lightcone wavefunctions.

In this paper, we analyse in a similar vein the corresponding lightcone boundstate Schrodinger equation for coarse transverse lattice gauge theory at large- N_c . By demanding finiteness of the boundstate energy, we determine the form of meson wavefunctions at small lightcone momentum. These depend on two exponents, α and β , whose values are independent of all details of the wavefunctions, which encode the leading non-analytic behaviour. In general, naive intuition based on the free lightcone kinetic energy is wrong. In particular, wavefunctions become more singular as more momenta vanish. Quark distributions diverge as $x \rightarrow 0$ and all Fock sectors contribute as $x \rightarrow 1$.

In the next section, we briefly review the colour-dielectric formulation of transverse lattice gauge theory and set up the boundstate Schrodinger equation to lowest non-trivial order of the colour-dielectric expansion that is used in the following two sections. Sections 3 and 4 determine systematically the behaviour of lightcone wavefunctions of mesons at small parton lightcone momentum. At first, in section 3, we use the approximation where up to one gauge link-variable is allowed in a state. Then, in section 4, we relax this approximation and generalise many of the results, giving a simple ansatz that incorporates all the boundary conditions. Applications of the results to the behaviour of quark generalised parton distributions are given in Section 5 and conclusions are discussed in Section 6.

2. REVIEW OF TRANSVERSE LATTICES

We introduce continuum light-cone co-ordinates $x^\pm = (x^0 \pm x^3)/\sqrt{2}$ and discretize the transverse coordinates $\mathbf{x} = (x^1, x^2)$ on a square lattice of spacing a . Lorentz indices μ, ν are split into light-cone indices $\alpha, \beta \in \{+, -\}$ and transverse indices $r, s \in \{1, 2\}$. Quark fields $\Psi(x^+, x^-, \mathbf{x})$ in the fundamental representation and longitudinal gauge potentials $A_\alpha(x^+, x^-, \mathbf{x})$ in the adjoint representation of the gauge group $SU(N_c)$ are associated to the sites of the transverse lattice. Flux link fields $M_r(x^+, x^-, \mathbf{x})$, which we choose to be in a complex matrix representation of $SU(N_c)$, are associated with the directed link from \mathbf{x} to $\mathbf{x} + a\hat{\mathbf{r}}$, where $\hat{\mathbf{r}}$ is a unit vector in direction r . In the transverse continuum limit $a \rightarrow 0$, these would be related to transverse gauge potentials $A_r(x^+, x^-, \mathbf{x})$. Subsequent analysis is done to leading order of the $1/N_c$ expansion, which allows one to drop the site argument \mathbf{x} of the fields [5, 6].

A. Lightcone Hamiltonian

For finite transverse lattice spacing a , the Lagrangian may contain any operator invariant under transverse lattice gauge symmetries, Poincaré symmetries manifestly preserved by the lattice cut-off, and renormalisable by dimensional counting with respect to the continuum co-ordinates x^α . One may control the subsequent proliferation of operators either by approaching the transverse continuum limit, in which case only renormalisable operators with respect to co-ordinates \mathbf{x} survive, or by ‘strong-coupling’ methods on a coarse lattice, such as the colour-dielectric expansion [5]. All calculations to date have used the colour-dielectric form [2] and it is this approach that we analyse here. This involves fixing to the light-cone gauge $A_- = 0$, classically eliminating non-dynamical fields A_+ , $\gamma^-\Psi$, then expanding the resulting lightcone Hamiltonian in powers of the remaining dynamical fields M_r , $\gamma^+\Psi$. Truncation of such an expansion is a valid approximation provided wavefunctions of interest (typically those of the lightest eigenstates) are dominated by few-body Fock states. This is achieved by the choice of sufficiently large masses for the dynamical fields. When the remaining couplings in the truncated hamiltonian are tuned to optimise symmetries broken by the lattice cutoff, the choice of large masses corresponds to choice of a coarse lattice spacing a .

The Lagrangian density L we consider, which was previously investigated in Ref. [7], contains all allowed terms up to order M^4 and $\bar{\Psi}M\Psi$. (There are additional terms involving multiple traces of products of M fields that contribute only to the glueball sector at large- N_c [8].)

$$\begin{aligned}
L = & \sum_{\alpha, \beta=+, -} \sum_{r=1, 2} -\frac{1}{2G^2} \text{Tr}\{F^{\alpha\beta}F_{\alpha\beta}\} + \text{Tr}\{[(\partial_\alpha + iA_\alpha)M_r - iM_rA_\alpha][\text{h.c.}]\} \\
& -\mu_b^2 \text{Tr}\{M_rM_r^\dagger\} - V[M] + i\bar{\Psi}\gamma^\alpha(\partial_\alpha + iA_\alpha)\Psi - \mu_f\bar{\Psi}\Psi \\
& + i\kappa_a(\bar{\Psi}\gamma^rM_r\Psi - \bar{\Psi}\gamma^rM_r^\dagger\Psi) + \kappa_s(\bar{\Psi}M_r\Psi + \bar{\Psi}M_r^\dagger\Psi) ,
\end{aligned} \tag{1}$$

where $F^{\alpha\beta}(\mathbf{x})$ is the continuum field strength in the (x^0, x^3) plane and the link-field

potential is

$$\begin{aligned}
V[M] = & -\frac{\beta}{a^2 N_c} \sum_{r \neq s} \text{Tr}\{M_r M_s M_r^\dagger M_s^\dagger\} + \frac{\lambda_1}{a^2 N_c} \sum_r \text{Tr}\{M_r M_r^\dagger M_r M_r^\dagger\} \\
& + \frac{\lambda_2}{a^2 N_c} \sum_r \text{Tr}\{M_r M_r M_r^\dagger M_r^\dagger\} + \frac{\lambda_4}{a^2 N_c} \sum_{\sigma=\pm 2, \sigma'=\pm 1} \text{Tr}\{M_\sigma^\dagger M_\sigma M_{\sigma'}^\dagger M_{\sigma'}\} . \quad (2)
\end{aligned}$$

We have defined $M_r = M_{-r}^\dagger$ and hold $G\sqrt{N_c}$, $\kappa_a\sqrt{N_c}$, and $\kappa_s\sqrt{N_c}$ finite as $N_c \rightarrow \infty$.

In the chiral representation,

$$\Psi = \frac{1}{2^{1/4}} \begin{pmatrix} u_+ \\ v_+ \\ v_- \\ u_- \end{pmatrix} \quad (3)$$

decomposes into two-dimensional complex spinors

$$u = \begin{pmatrix} u_+ \\ u_- \end{pmatrix} \quad v = \begin{pmatrix} v_+ \\ v_- \end{pmatrix} . \quad (4)$$

The helicity subscript $h = \pm$ denotes the sign of the eigenvalue of γ^5 . Using Pauli matrices, we may then write various bilinears

$$\bar{\Psi}\Psi = -\frac{1}{\sqrt{2}} (u^\dagger \sigma^1 v + v^\dagger \sigma^1 u) \quad (5)$$

$$\bar{\Psi}\gamma^+\Psi = u^\dagger u \quad (6)$$

$$\bar{\Psi}\gamma^-\Psi = v^\dagger v \quad (7)$$

$$\bar{\Psi}\gamma^1\Psi = \frac{1}{\sqrt{2}} (u^\dagger \sigma^3 v + v^\dagger \sigma^3 u) \quad (8)$$

$$\bar{\Psi}\gamma^2\Psi = \frac{i}{\sqrt{2}} (v^\dagger u - u^\dagger v) \quad (9)$$

$$\bar{\Psi}\gamma_5\Psi = \frac{i}{\sqrt{2}} (v^\dagger \sigma^2 u + u^\dagger \sigma^2 v) . \quad (10)$$

We also introduce the matrices ζ^λ which act on the 2-spinors:

$$\frac{\lambda}{\zeta^\lambda} \begin{vmatrix} 1 & 2 & -1 & -2 \\ \sigma^2 & -\sigma^1 & -\sigma^2 & \sigma^1 \end{vmatrix} . \quad (11)$$

In light-cone gauge $A_- = 0$, A_+ and v are non-dynamical (independent of light-cone time x^+) and their constraint equations of motion are used to eliminate them at the

classical level. The lightcone Hamiltonian may then be obtained from the action (1) in the standard way in terms of the remaining dynamical fields u , M_1 , and M_2 . If we define

$$F = -u + \sum_{\lambda} M_{\lambda} \left(\frac{\kappa_s}{\mu_f} + i \frac{\kappa_a}{\mu_f} \zeta^{\lambda} \right) u , \quad (12)$$

$$J^+ = uu^{\dagger} + i \sum_{\lambda} M_{\lambda} \overset{\leftrightarrow}{\partial}_- M_{\lambda}^{\dagger} , \quad (13)$$

the lightcone Hamiltonian one finds is

$$\begin{aligned} P^- = & \int dx^- \frac{G^2}{4} \text{Tr} \left\{ J^+ \frac{1}{(i\partial_-)^2} J^+ \right\} - \frac{G^2}{4N_c} \text{Tr} \{ J^+ \} \frac{1}{(i\partial_-)^2} \text{Tr} \{ J^+ \} \\ & + \frac{\mu_f^2}{2} F^{\dagger} \frac{1}{i\partial_-} F + V[M] . \end{aligned} \quad (14)$$

Under certain reasonable assumptions [9], the Hamiltonian (14) is a truncation of the most general Hamiltonian to order M^4 and $u^2 M$. It also contains some, but not all, allowed operators at order $u^2 M^2$ and u^4 ; most importantly, it contains those responsible for confinement [1].

B. Fock space

Introducing the mode expansions

$$\begin{aligned} M_r(x^+ = 0, x^-) &= \frac{1}{\sqrt{4\pi}} \int_0^{\infty} \frac{dk^+}{\sqrt{k^+}} \left(a_{-r}(k^+) e^{-ik^+ x^-} + a_r^{\dagger}(k^+) e^{ik^+ x^-} \right) , \\ u(x^+ = 0, x^-) &= \frac{1}{\sqrt{2\pi}} \int_0^{\infty} dk^+ \left(b(k^+) e^{-ik^+ x^-} + \sigma^1 d^{\dagger}(k^+) e^{ik^+ x^-} \right) , \end{aligned} \quad (15)$$

we have

$$\left[a_{\lambda,ij}(k^+), a_{\rho,kl}^*(\tilde{k}^+) \right] = \delta_{ik} \delta_{jl} \delta_{\lambda\rho} \delta(k^+ - \tilde{k}^+) , \quad (16)$$

$$\left[a_{\lambda,ij}(k^+), a_{\rho,kl}(\tilde{k}^+) \right] = 0 , \quad (17)$$

$$\left\{ b_{h,i}(k^+), b_{h',j}^*(\tilde{k}^+) \right\} = \delta_{ij} \delta_{hh'} \delta(k^+ - \tilde{k}^+) , \quad (18)$$

$$\left\{ b_{h,i}(k^+), b_{h',j}(\tilde{k}^+) \right\} = 0 , \quad (19)$$

where i, j are colour indices, λ and $\rho \in \{\pm 1, \pm 2\}$ denote the orientations of link variables in the (x^1, x^2) plane, and $(a_{\lambda,ij})^* = (a_{\lambda}^{\dagger})_{ji}$. The sequence of orientations $\{\lambda_2, \dots, \lambda_{n-1}\}$ of link variables together with the P^+ momentum fractions $x_a = k_a^+/P^+$ and quark helicities h, h' are sufficient to encode the structure of Fock states contributing to the boundstate at zero total transverse momentum $\mathbf{P} = \mathbf{0}$. Only gauge singlet combinations under residual gauge transformations in $A_- = 0$ gauge can contribute to states of finite

energy [1], so a boundstate containing quarks at large N_c decomposes in terms of Fock states as

$$\begin{aligned}
|\psi(P^+)\rangle = & \sum_{n=2}^{\infty} \sum_{h, \lambda_2, \dots, \lambda_{n-1}, h'} 2\sqrt{\pi N_c} \left(\frac{P^+}{N_c}\right)^{n/2} \int_0^{P^+} dx_1 \cdots dx_n \delta\left(1 - \sum_{a=1}^n x_a\right) \\
& \times \psi_n(x_1, \dots, x_n; h, \lambda_2, \dots, \lambda_{n-1}, h') \\
& \times b_h^\dagger(x_1 P^+) a_{\lambda_2}^\dagger(x_2 P^+) \cdots a_{\lambda_{n-1}}^\dagger(x_{n-1} P^+) d_{h'}^*(x_n P^+) |0\rangle.
\end{aligned} \tag{20}$$

The state is normalised by

$$1 = \sum_{n=2}^{\infty} \sum_{h, \lambda_2, \dots, \lambda_{n-1}, h'} \int_0^1 dx_1 \cdots dx_n \delta\left(1 - \sum_{a=1}^n x_a\right) |\psi_n|^2 \tag{21}$$

if

$$\langle \psi(P_1^+) | \psi(P_2^+) \rangle = 2P_1^+ (2\pi) \delta(P_1^+ - P_2^+). \tag{22}$$

The object of this paper is to determine the behaviour of the wavefunctions $\psi_n(x_1, \dots)$ when one or more x_a are small. The Fock space matrix elements of the invariant mass operator $2P^+P^-$ resulting from (14) were given in Ref. [7]. For ease of reference and to correct some typing errors in interaction (ii), we reproduce these in a slightly more efficient notation as Fig. 5 and Table II in Appendix A. Projecting $2P^+P^-|\psi(P^+)\rangle = \mathcal{M}^2|\psi(P^+)\rangle$, where \mathcal{M} is the invariant mass eigenvalue, onto individual Fock states, one obtains integral equations for the wavefunctions.

3. ONE-LINK APPROXIMATION

To begin analysing the small x behaviour of the boundstate equations, we make the approximation of restricting the sum in Eq. (20) to $n \leq 3$, i.e. at most one flux link in a state. We correspondingly restrict to interactions (i)(ii)(iii)(vii)(viii) (see Appendix A). The π or η' meson state can then be written as

$$\begin{aligned}
|\psi(P^+)\rangle = & 2\sqrt{\frac{\pi}{N_c}} P^+ \int_0^1 dx \psi(x) b^\dagger(x P^+) \sigma^2 d^\dagger((1-x)P^+) |0\rangle \\
& + \frac{2\sqrt{\pi}(P^+)^{3/2}}{N_c} \int_0^1 dx \int_0^{1-x} dy \sum_{\lambda} \left\{ \psi_S(x, y) b^\dagger(x P^+) \sigma^2 a_\lambda^\dagger(y P^+) d^\dagger((1-x-y)P^+) \right. \\
& \left. + \psi_A(x, y) b^\dagger(x P^+) \zeta^\lambda \sigma^2 a_\lambda^\dagger(y P^+) d^\dagger((1-x-y)P^+) \right\} |0\rangle.
\end{aligned} \tag{23}$$

To obtain the $\mathcal{J}_3 = 0$ spin projection component of the ρ meson, one replaces $\sigma^2 \rightarrow \sigma^1$ in the above. The wavefunctions of the $\mathcal{J}_3 = \pm 1$ components of the ρ meson are more

complicated:

$$\begin{aligned}
|\psi(P^+)\rangle = & 2\sqrt{\frac{\pi}{N_c}}P^+ \int_0^1 dx \psi(x) b^\dagger(xP^+) \sigma^3 d^\dagger((1-x)P^+) |0\rangle \\
& + \frac{2\sqrt{\pi}(P^+)^{3/2}}{N_c} \int_0^1 dx \int_0^{1-x} dy \sum_\lambda \left\{ \psi_S(x, y) b^\dagger(xP^+) \sigma^3 a_\lambda^\dagger(yP^+) d^\dagger((1-x-y)P^+) \right. \\
& + \psi_A(x, y) b^\dagger(xP^+) \zeta^\lambda \sigma^3 a_\lambda^\dagger(yP^+) d^\dagger((1-x-y)P^+) \\
& \left. + \psi'_A(x, y) b^\dagger(xP^+) \sigma^1 \zeta^\lambda \sigma^1 \sigma^3 a_\lambda^\dagger(yP^+) d^\dagger((1-x-y)P^+) \right\} |0\rangle. \tag{24}
\end{aligned}$$

This is the state that is odd under reflections \mathcal{P}^1 : $x^1 \rightarrow -x^1$; the even state is obtained by removing the σ^3 .

The bound state equations for these four states are almost identical. The $n = 2$ bound state equation is

$$\begin{aligned}
\mathcal{M}^2 \psi(x) = & \frac{\mu_f^2}{x(1-x)} \psi(x) + \frac{(\kappa_s^2 + \kappa_a^2)N_c}{\pi} \left[\int_0^x \frac{dy}{xy} + \int_0^{1-x} \frac{dy}{(1-x)y} \right] \psi(x) \\
& - \frac{G^2 N_c}{2\pi} \int_0^1 \frac{dy}{(x-y)^2} (\psi(y) - \psi(x)) \\
& - \frac{\mu_f \kappa_s \sqrt{N_c}}{\sqrt{\pi}} \left[\int_0^x dy \frac{(2x-y) \psi_S(x-y, y)}{\sqrt{y} x(x-y)} + \int_0^{1-x} dy \frac{(2-2x-y) \psi_S(x, y)}{\sqrt{y}(1-x)(1-x-y)} \right] \\
& + \frac{\mu_f \kappa_a \sqrt{N_c}}{\sqrt{\pi}} \left[\int_0^x dy \frac{\sqrt{y} \psi_A(x-y, y)}{x(x-y)} \right. \\
& \left. + \int_0^{1-x} dy \frac{\sqrt{y}}{(1-x)(1-x-y)} \begin{cases} \psi_A(x, y) & \text{for pion} \\ -\psi_A(x, y) & \text{for rho, } \mathcal{J}_3 = 0 \\ -\psi'_A(x, y) & \text{for rho, } \mathcal{J}_3 = \pm 1 \end{cases} \right]. \tag{25}
\end{aligned}$$

For each of the wavefunctions, ψ_S , ψ_A , ψ'_A , the $n = 3$ bound state equation is

$$\begin{aligned}
\mathcal{M}^2 \psi(x, y) = & \mu_f^2 \left(\frac{1}{x} + \frac{1}{1-x-y} \right) \psi(x, y) + \frac{\mu_b^2}{y} \psi(x, y) \\
& - \frac{G^2 N_c}{4\pi} \left[\int_0^{x+y} dz \frac{y+z}{\sqrt{yz}(y-z)^2} \psi(x+y-z, z) \right. \\
& + \int_0^{1-x} dz \frac{y+z}{\sqrt{yz}(y-z)^2} \psi(x, z) \\
& \left. - 2\psi(x, y) \left(\frac{2}{y} + \int_0^{x+y} \frac{dz}{(y-z)^2} + \int_0^{1-x} \frac{dz}{(y-z)^2} \right) \right]. \tag{26}
\end{aligned}$$

For $\psi_S(x, y)$, we include

$$- \frac{\mu_f \kappa_s \sqrt{N_c}}{\sqrt{\pi y}} \left[\frac{2x+y}{x(x+y)} \psi(x+y) + \frac{2-2x-y}{(1-x)(1-x-y)} \psi(x) \right]. \tag{27}$$

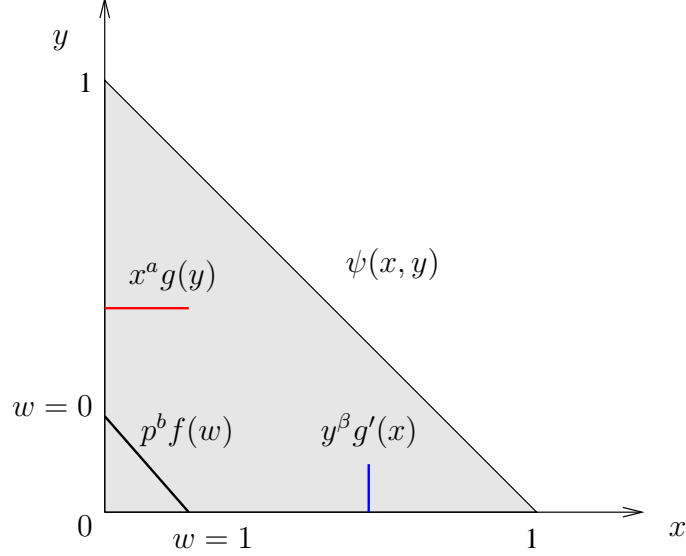


FIG. 1: The $n = 3$ wavefunction $\psi(x, y)$ in the limits $x \rightarrow 0$, $y \rightarrow 0$, or $p = x + y \rightarrow 0$.

For $\psi_A(x, y)$ in the pion and the rho $\mathcal{J}_3 = 0$ state, we include

$$+ \frac{\mu_f \kappa_a \sqrt{N_c y}}{\sqrt{\pi}} \left[\frac{\psi(x+y)}{x(x+y)} + \frac{1}{(1-x)(1-x-y)} \begin{cases} \psi(x) & \text{for pion} \\ -\psi(x) & \text{for rho} \end{cases} \right]. \quad (28)$$

For $\psi_A(x, y)$ in the rho $\mathcal{J}_3 = \pm 1$ states, we include

$$+ \frac{\mu_f \kappa_a \sqrt{N_c y} \psi(x+y)}{\sqrt{\pi} x(x+y)}. \quad (29)$$

For $\psi'_A(x, y)$ in the rho $\mathcal{J}_3 = \pm 1$ states, we include

$$- \frac{\mu_f \kappa_a \sqrt{N_c y} \psi(x)}{\sqrt{\pi} (1-x)(1-x-y)}. \quad (30)$$

Next, we analyze the singularities as one or more of the momenta go to zero. We will consider each of the following limits:

$$\lim_{x \rightarrow 0} \psi(x) = C_2 x^\alpha \quad (31)$$

$$\lim_{\substack{x \rightarrow 0, \\ y \text{ constant}}} \psi(x, y) = x^a g(y) \quad (32)$$

$$\lim_{\substack{y \rightarrow 0, \\ x \text{ constant}}} \psi(x, y) = y^\beta g'(x) \quad (33)$$

$$\lim_{\substack{x+y \rightarrow 0, \\ x/y \text{ constant}}} \psi(x, y) = (x+y)^b f\left(\frac{x}{x+y}\right) = p^b f(w), \quad (34)$$

where $x = wp$, and $y = (1-w)p$. See Figure 1. The remaining limit of interest, $1-x \rightarrow 0$ with $(1-x)/y$ constant, is equivalent to the limit (34) by charge conjugation.

A. $n = 3$ equation, limit $x \rightarrow 0$:

For $\psi_S(x, y)$, we obtain:

$$\begin{aligned}
0 = & \mu_f^2 g_S(y) x^{a-1} - \frac{\mu_f \kappa_s \sqrt{N_c}}{\sqrt{\pi y}} \psi(y) x^{-1} \\
& - \frac{G^2 N_c}{4\pi} \int_0^{x+y} \frac{dz}{(y-z)^2} \left[\frac{y+z}{\sqrt{yz}} \psi(x+y-z) - 2\psi(x, y) \right] \\
& + O(x^a) .
\end{aligned} \tag{35}$$

For $\psi_A(x, y)$, we obtain:

$$\begin{aligned}
0 = & \mu_f^2 g_A(y) x^{a-1} + \frac{\mu_f \kappa_a \sqrt{N_c}}{\sqrt{\pi y}} \psi(y) x^{-1} \\
& - \frac{G^2 N_c}{4\pi} \int_0^{x+y} \frac{dz}{(y-z)^2} \left[\frac{y+z}{\sqrt{yz}} \psi(x+y-z) - 2\psi(x, y) \right] \\
& + O(x^a) .
\end{aligned} \tag{36}$$

In order to cancel the divergence of second term, we must set $a = 0$. We then find that the integral term, which is also $O(x^{a-1})$, goes to zero. Simplifying, we get:

$$\lim_{x \rightarrow 0} \psi_S(x, y) = \frac{\kappa_s \sqrt{N_c}}{\mu_f \sqrt{\pi y}} \psi(y) \tag{37}$$

$$\lim_{x \rightarrow 0} \psi_A(x, y) = - \frac{\kappa_a \sqrt{N_c}}{\mu_f \sqrt{\pi y}} \psi(y) . \tag{38}$$

B. $n = 3$ equation, limit $y \rightarrow 0$:

For this limit, the resulting equation is the same for ψ_S and ψ_A because the differing terms are non-leading.

$$\begin{aligned}
0 = & \left(\mu_b^2 + \frac{G^2 N_c}{\pi} \right) g'(x) y^{\beta-1} \\
& - \frac{G^2 N_c}{4\pi} y^{-1} \int_0^{1/y} \frac{dq}{(1-q)^2} \left[\frac{1+q}{\sqrt{q}} (qy)^\beta g'(x) - 2y^\beta g'(x) \right] \\
& + O(y^{-\frac{1}{2}}) .
\end{aligned} \tag{39}$$

We find the constraint $\beta < \frac{1}{2}$, so that the integrals converge, in which case the $O(y^{-\frac{1}{2}})$ terms are non-leading. We also have the constraint $\beta > 0$, so that the expectation value of $2P^+ P^-$ is finite. Thus, we obtain:

$$0 = \left(\mu_b^2 + \frac{G^2 N_c}{\pi} \right) g'(x) y^{\beta-1} - \frac{G^2 N_c}{4\pi} g'(x) y^{\beta-1} 2 [2\pi\beta \tan(\pi\beta) + 2] . \tag{40}$$

Simplifying, we derive:

$$0 = [\mu_b^2 - G^2 N_c \beta \tan(\pi\beta)] g'(x) y^{\beta-1}. \quad (41)$$

Note that $g'(x)$ is not fixed by this analysis. Eq. (41) is the same expression that one obtains for the two-link bound state equation without quarks [1].

C. $n = 3$ equation, limit $x + y \rightarrow 0$, x/y constant

In this limit, we obtain, for both $f_S(w)$ and $f_A(w)$:

$$\begin{aligned} 0 = & \frac{\mu_f^2 f(w)}{w} p^{b-1} + \frac{(\mu_b^2 + \frac{G^2 N_c}{\pi}) f(w)}{1-w} p^{b-1} \\ & - \frac{G^2 N_c}{4\pi} p^{b-1} \int_0^1 \frac{dq}{(q-w)^2} \left[\frac{(2-w-q) f(q)}{\sqrt{(1-w)(1-q)}} - 2 f(w) \right] \\ & - \frac{G^2 N_c}{4\pi} p^{b-1} \int_0^1 \frac{dq}{(q-w)^2} \left[\frac{(w+q-2qw) f(q)}{\sqrt{(1-w)(1-q)}} \left(\frac{w}{q} \right)^\alpha - 2w f(w) \right] \\ & + \frac{\mu_f C_2 \sqrt{N_c}}{\sqrt{\pi} w} p^{\alpha-3/2} \begin{cases} -\kappa_s \frac{(w+1)}{\sqrt{1-w}} & \text{for } f_S(w) \\ \kappa_a \sqrt{1-w} & \text{for } f_A(w) \end{cases} \\ & + O(p^{-1/2}) . \end{aligned} \quad (42)$$

In order for the last term in the equation to be cancelled in the limit $p \rightarrow 0$, we must set $b = \alpha - \frac{1}{2}$. Thus,

$$\lim_{x+y \rightarrow 0} \psi(x, y) = p^{\alpha-1/2} f(w) . \quad (43)$$

D. $n = 2$ equation, limit $x \rightarrow 0$:

Taking the $x \rightarrow 0$ limit of Eq. (25) and using (43), we obtain

$$\begin{aligned} 0 = & \mu_f^2 C_2 x^{\alpha-1} - \frac{G^2 N_c C_2}{2\pi} (1 - \pi\alpha \cot(\pi\alpha)) x^{\alpha-1} \\ & + x^{\alpha-1} \int_0^1 \frac{dz}{1-z} \left[\frac{\kappa_s^2 N_c C_2}{\pi} - \frac{\mu_f \kappa_s \sqrt{N_c}}{\sqrt{\pi}} \left(\frac{(2-z) f_S(1-z)}{\sqrt{z}} \right) \right] \\ & + x^{\alpha-1} \int_0^1 \frac{dz}{1-z} \left[\frac{\kappa_a^2 N_c C_2}{\pi} + \frac{\mu_f \kappa_a \sqrt{N_c}}{\sqrt{\pi}} (\sqrt{z} f_A(1-z)) \right] \\ & + O(x^0) . \end{aligned} \quad (44)$$

For the expectation value of the energy to be finite, we must have $0 \leq \alpha < 1$.

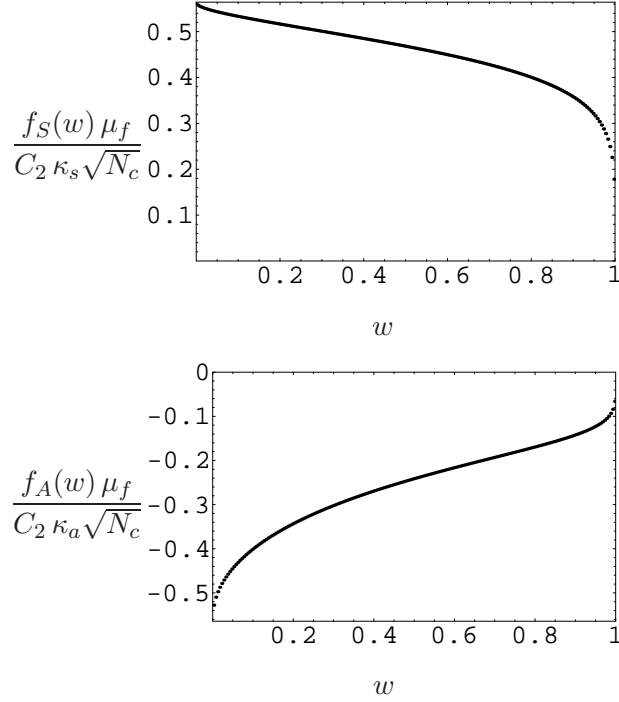


FIG. 2: $f_S(w)$ and $f_A(w)$ vs. w for couplings $\mu_f = 0.362G\sqrt{N_c}$, $\mu_b = 0.2G\sqrt{N_c}$, and $\alpha = 0.4$.

E. Self-consistent solution

To determine α , one must find $f_S(w)/C_2$ and $f_A(w)/C_2$ that self-consistently solve Equations (42) and (44). We obtained solutions numerically by discretizing w on the interval $[0,1]$. Using numerical calculations of $f_S(w)/C_2$ and $f_A(w)/C_2$, one can study the dependence of α on the couplings in the Hamiltonian; see Figures 3–4. Note that α is very nearly constant with respect to link field mass μ_b (Fig. 3). Also, note that α is outside of its allowed range for some areas of the coupling space, corresponding generally to large values of $\kappa_s\sqrt{N_c}$ and $\kappa_a\sqrt{N_c}$ (Fig. 4). Thus, the endpoint behavior of the wavefunction can restrict the allowed values of the couplings.

4. BEYOND ONE LINK

When relaxing the truncation on n and including the other interactions of Fig. 5, most of the complication occurs in the analytic auxiliary functions, such as f , g , g' in the previous section. If we wish to determine only the form of the leading non-analytic behaviour of wavefunctions at small momenta, the analysis is somewhat simpler. We note that this is independent of spin, represented by quark helicity and link field transverse orientation. Consider the effect of including $n = 4$ wavefunctions ψ_4 and the other interactions of Fig. 5. In the following we ignore the spin dependence, finding only the momentum dependent part of these contributions. Accordingly, we label wavefunction

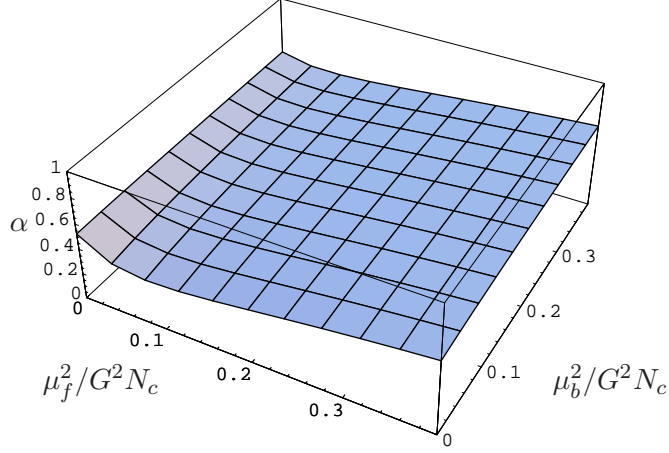


FIG. 3: α vs. μ_f^2 and μ_b^2 , $\kappa_s = -0.323G$, $\kappa_a = 0.162G$.

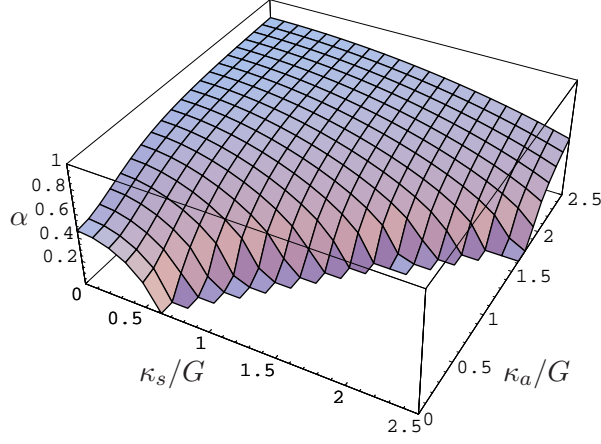


FIG. 4: α vs. κ_s/G and κ_a/G ; $\mu_f = 0.362G\sqrt{N_c}$, and $\mu_b = 0.2G\sqrt{N_c}$.

components ψ_n by the number of partons n and their lightcone momenta only.

A. $n = 2$ equation

To the $n = 2$ boundstate equation (25) we must add interactions $(iv)(vi)$:

$$\int dydz \frac{y-z}{4\pi(y+z)^2\sqrt{yz}} \psi_4(x-y-z, y, z) + \text{antiquarks} \quad (45)$$

from (iv) , and

$$\int dydz \frac{1}{4\pi(x-z)\sqrt{yz}} \psi_4(x-y-z, y, z) + \text{antiquarks} \quad (46)$$

from (vi). If we assume that these contribute at the leading $x^{\alpha-1}$ order as $x \rightarrow 0$ in the analysis of Section 3 D, then

$$\psi_4(x, y, z) \sim (1-x)^{\alpha-1} \text{ as } x \rightarrow 1 . \quad (47)$$

B. $n = 3$ equation

In the $n = 3$ equation (26), we must include interaction (v), that connects $n = 3$ to $n = 3$ and was previously omitted:

$$\int dz \frac{1}{4\pi(x+y)\sqrt{yz}} \psi_3(x+y-z, z) + \text{antiquarks} . \quad (48)$$

This is subleading in the $x \rightarrow 0$ analysis of Section 3 A and the $y \rightarrow 0$ analysis of Section 3 B (recall that $\beta < 1/2$). It contributes at the leading order p^{b-1} in the analysis of Section 3 C, but does not affect the relation $b = \alpha - \frac{1}{2}$. To the $n = 3$ equation (26) we must also add terms involving ψ_4 via interaction (ii):

$$\int dz \frac{1}{2\sqrt{\pi z}} \left(\frac{1}{x} \pm \frac{1}{x-z} \right) \psi_4(x-z, z, y) . \quad (49)$$

If we assume that these contribute at the leading x^{-1} order of the analysis in Section 3 A, then

$$\psi_4(wp, (1-w)p, z) \sim p^{-1/2} \text{ as } p \rightarrow 0 . \quad (50)$$

In the $y \rightarrow 0$ analysis of Section 3 B, (49) does not contribute at leading order since, by normalisability, $\beta - 1 < -1/2$ and $\psi_4(x-z, z, y)$ cannot diverge faster than $1/\sqrt{y}$ when $y \rightarrow 0$. In the analysis of Section 3 C, property (47) implies that (49) contributes at the leading $p^{\alpha-3/2}$ order as $p \rightarrow 0$.

C. $n = 4$ equation

Finally, there will be a new $n = 4$ boundstate equation for $\mathcal{M}^2 \psi_4(x, y, z)$. The momentum dependent parts of these contributions are given in Table I.

Repeating the analysis of Sections 3 A and 3 B for $n = 4$, we again find from comparing interactions (i) and (ii) that

$$\psi_4(x, y, z) \sim x^0 \text{ as } x \rightarrow 0 , \quad (51)$$

since all other interactions are subleading, while from interactions (viii)(ix)

$$\psi_4(x, y, z) \sim y^\beta \text{ as } y \rightarrow 0 . \quad (52)$$

We confirm directly, from the $n = 4$ amplitudes of Table I, the correctness of Eq. (50) and Eq. (47), thus verifying the assumptions that went into deriving them. In a similar

TABLE I: The momentum dependent parts of interactions contributing to the boundstate equation for $\mathcal{M}^2\psi_4(x, y, z)$.

$\frac{1}{x}\psi_4(x, y, z) + \text{antiquarks}$	(i)
$\frac{1}{2\sqrt{\pi y}} \left(\frac{1}{x} \pm \frac{1}{x+y} \right) \psi_3(x+y, z) + \text{antiquarks}$	(ii)
$\frac{(y-z)\psi_2(x+y+z)}{4\pi(y+z)^2\sqrt{yz}} + \text{antiquarks}$	(iv)
$\int dv \frac{\psi_4(x+y-v, v, z)}{4\pi(x+y)\sqrt{yv}} + \text{antiquarks}$	(v)
$\frac{\psi_2(x+y+z)}{4\pi(x+y)\sqrt{yz}} + \text{antiquarks}$	(vi)
$\left(\frac{1}{y} + \frac{1}{z} \right) \psi_4(x, y, z)$	(vii)
$\frac{-1}{4\pi} P \int dv \frac{(y+v)\psi_4(x+y-v, v, z)}{\sqrt{vy}(v-y)^2} + \text{antiquarks}$	(viii)
$\frac{-1}{8\pi} P \int dv \frac{(v+z)(2y+z-v)\psi_4(x, y+z-v, v)}{\sqrt{yzv}(y+z-v)(z-v)^2}$	(ix)
$\int dv \frac{\psi_4(x, y+z-v, v)}{4\pi\sqrt{yzv}(y+z-v)}$	(x)
$\frac{-1}{8\pi} \int dv \frac{(y-z)(y+z-2v)}{\sqrt{yzv}(y+z-v)(z+y)^2} \psi_4(x, y+z-v, v)$	(xiii)

way we also deduce as $p \rightarrow 0$:

$$\psi_4(x, wp, (1-w)p) \sim p^0 \quad (53)$$

$$\psi_4(wp, y, (1-w)p) \sim p^\beta \quad (54)$$

$$\psi_4(wp, y, 1-y-p) \sim p^0 \quad (55)$$

and

$$\psi_4(x, y, z) \sim (1-y)^{\alpha-1/2} \text{ as } y \rightarrow 1 \quad (56)$$

D. Summary

We can summarize all these results in the following forms for ψ_n , which have the correct endpoint behaviour when any number of momenta vanish:

$$\begin{aligned}
\psi_2(x) &= C_2 x^\alpha (1-x)^\alpha \\
\psi_3(x, y) &= C_3 \frac{y^\beta (1-y)^\alpha}{[(x+y)(1-x)]^{\beta-\alpha+1/2}} \\
\psi_4(x, y, z) &= C_4 \frac{(yz)^\beta [(1-y)(1-z)]^\alpha [(x+y+z)(1-x)]^{\alpha+\beta-1/2}}{[(x+y)(1-x-y)]^{\beta+1/2} (y+z)^{2\beta}}
\end{aligned} \quad (57)$$

The exponents α and β are independent of n , quark helicity, and the transverse shape, while the auxiliary functions C_n are dependent on all of these factors. If the C_n are made from a complete set of functions of x_a , non-singular in the limit when any number of momenta vanish, then any boundstate wavefunction should be expressible in the form (57).

We have also examined the effect of higher orders in $n \geq 5$. The forms (57) remain invariant, although the exponents α and β are renormalised in general because of parton self-energy and vacuum polarization. Wavefunctions ψ_n analogous to (57) become increasingly complicated at higher n and we have not found a simple general expression; no new exponents beyond α and β occur however. Of special interest are the limits

$$\psi_n(x_1, x_2, \dots) \sim (1 - x_1)^{\alpha - (n-2)/2} \text{ as } x_1 \rightarrow 1 \quad (58)$$

$$\psi_n(x_1, x_2, \dots) \sim (x_1)^0 \text{ as } x_1 \rightarrow 0 \quad (59)$$

which follow from comparing interactions (i) and (ii). These govern the behaviour of hadronic structure functions at large and small Bjorken x , as discussed in Section 5.

The forms (57) demonstrate that lightcone wavefunctions become more singular as more lightcone momenta vanish, even though this is a ‘high-energy’ limit. Intuition from the free lightcone kinetic energy (sum of all terms (i) and (vii) in Table II of Appendix A) would have suggested the complete opposite. Rather than simply vanishing at the edges of phase space, as indicated by the free theory, the interactions have forced relations between wavefunctions with different numbers of partons to cancel divergences in the boundstate equations. This was noted for continuum QCD for a single vanishing x_a in Ref. [4], but for the transverse lattice we are able to generalise it to any number of vanishing momenta. Our analysis rules out a number of naive models for the lightcone wavefunctions, including products of individual parton wavefunctions and functions of the free kinetic energy.

5. APPLICATIONS

Based on the previous analysis, we can make definite statements about the behaviour of quark parton distributions in mesons at the edges of phase space. Some other recent studies of these distributions in various models have been made in Refs. [10]. We use the generalised quark distributions [11], which in lightcone gauge are defined as

$$\mathcal{H}(\bar{x}, \xi, Q^2) = \frac{1}{\sqrt{1 - \xi^2}} \int_{-\infty}^{+\infty} \frac{dz^-}{4\pi} e^{i\bar{x}\bar{P}^+ z^-} \langle P_{\text{in}} | \bar{\Psi}(-z^-/2) \gamma^+ \Psi(z^-/2) | P_{\text{out}} \rangle, \quad (60)$$

$$Q = P_{\text{in}} - P_{\text{out}} \quad (61)$$

$$\xi = \frac{(P_{\text{in}} - P_{\text{out}})^+}{2\bar{P}^+} \quad (62)$$

$$\bar{P}^+ = \frac{(P_{\text{in}} + P_{\text{out}})^+}{2}. \quad (63)$$

Bars generally indicate an average over in and out states. In Eq. (60), we define the boundstates at non-zero transverse momentum \mathbf{P} by boosting the Fock states with the Poincaré generators $\mathbf{M}^+ = (M^{+1}, M^{+2})$:

$$\begin{aligned} & \exp[-i\mathbf{M}^+ \cdot \mathbf{P}/P^+] b_h^\dagger(x_1 P^+) a_{\lambda_2}^\dagger(x_2 P^+) \cdots a_{\lambda_{n-1}}^\dagger(x_{n-1} P^+) d_{h'}^*(x_n P^+) |0\rangle \\ &= \exp[i\mathbf{P} \cdot \mathbf{c}] b_h^\dagger(x_1 P^+) a_{\lambda_2}^\dagger(x_2 P^+) \cdots a_{\lambda_{n-1}}^\dagger(x_{n-1} P^+) d_{h'}^*(x_n P^+) |0\rangle, \end{aligned} \quad (64)$$

$$\mathbf{c} = (c^1, c^2) = \sum_{a=1}^n x_a \mathbf{x}_a, \quad (65)$$

$$\mathbf{x}_{p+1} = \mathbf{x}_p + a \hat{\lambda}_{p+1}, \quad p = 1 \text{ to } n-2, \quad (66)$$

where $\hat{\lambda}_{p+1}$ is a transverse unit vector in the direction of the p^{th} link. The boundaries of interest are typically at large and small \bar{x} and at the transition point $\bar{x} = \xi$.

A. $\bar{x} \rightarrow 1$

We find from Eqs. (60) and (58) that each ψ_n contributes $\sim (1 - \bar{x})^{2\alpha}$ to $\mathcal{H}(\bar{x}, \xi, Q^2)$ as $\bar{x} \rightarrow 1$. This is interesting because the conventional wisdom, based upon the free kinetic energy, is that ψ_2 should dominate in this region — all but one parton has small momentum, so the free kinetic energy is minimized by the minimum number of partons. Although the exponent *is* correctly given by the lowest Fock wavefunction, which governs the distribution amplitude, on the transverse lattice all higher Fock states contribute to the structure function with the same power.

B. $x \rightarrow 0$

We find from Eqs. (60) and (59) that ψ_n contributes $\sim (\ln \frac{1}{x})^{n-3}$, $n > 2$, to the traditional quark distribution function $\mathcal{H}(x, 0, 0)$ as $x \rightarrow 0$. Thus, the sum over all Fock sectors n rises faster than any power of $\ln x$, i.e. at least like a power of x . This is consistent with the Regge behaviour of structure functions in the small- x region.

C. $\bar{x} \rightarrow \xi^+$

Unfortunately, we are not able to explore the region $\bar{x} < \xi$ with the strict large- N_c wavefunctions. That region is governed by their $1/N_c$ corrections, since it depends upon quark pair production. However, we find from Eq. (57) that ψ_2 contributes zero, while ψ_3 and ψ_4 contribute finite constants to $\mathcal{H}(\bar{x}, \xi, Q^2)$ as $\bar{x} \rightarrow \xi$ from above, provided $\xi > 0$. This is presumably true for higher n also and, provided these constants fall sufficiently rapidly with n , suggests that $\mathcal{H}(\xi, \xi, Q^2)$ is finite.

6. CONCLUSIONS

By demanding finiteness of the boundstate energy, we have determined the form (57) of meson wavefunctions at small lightcone momentum in a coarse transverse lattice gauge theory at large N_c . The forms depend on two exponents α and β , independent of the other details of the wavefunction such as spin and number of partons, which encode the leading non-analytic behaviour. As more momenta vanish, wavefunctions become more singular, contrary to the naive intuition from free lightcone kinetic energy, which diverges in these limits. The analytic forms lead to predictions for the behaviour near their endpoints of quark distributions. In particular, we see Regge behaviour at small x and contributions from all Fock states at large x .

The use of coarse lattice wavefunctions in transverse position space simplified the analysis, allowing us to separate the lightcone momentum problem from the transverse structure. The large- N_c limit also aided us by restricting the diagrammatic rules to planar ones and suppressing quark pair production. We would need to reformulate the problem at finite N_c in order to study the small lightcone momentum behaviour in baryons and in the sea quark part of wavefunctions. There is also the question of higher orders of the colour-dielectric expansion; that is, higher powers of dynamical quark and link fields in the lightcone hamiltonian. We have investigated some of these possible terms, but found none that altered the form (57), although the values of α and β are affected. Finally, it would be interesting to investigate similar questions in continuum lightcone QCD.

Acknowledgments

This work was supported in part by PPARC Visiting Fellowship grant PPA/V/S/2000/00513. The work of SD was supported by PPARC grant PPA/G/0/2002/00470. The work of JB, BvdS, & EW was supported by the Research Corporation.

APPENDIX A: INTERACTIONS

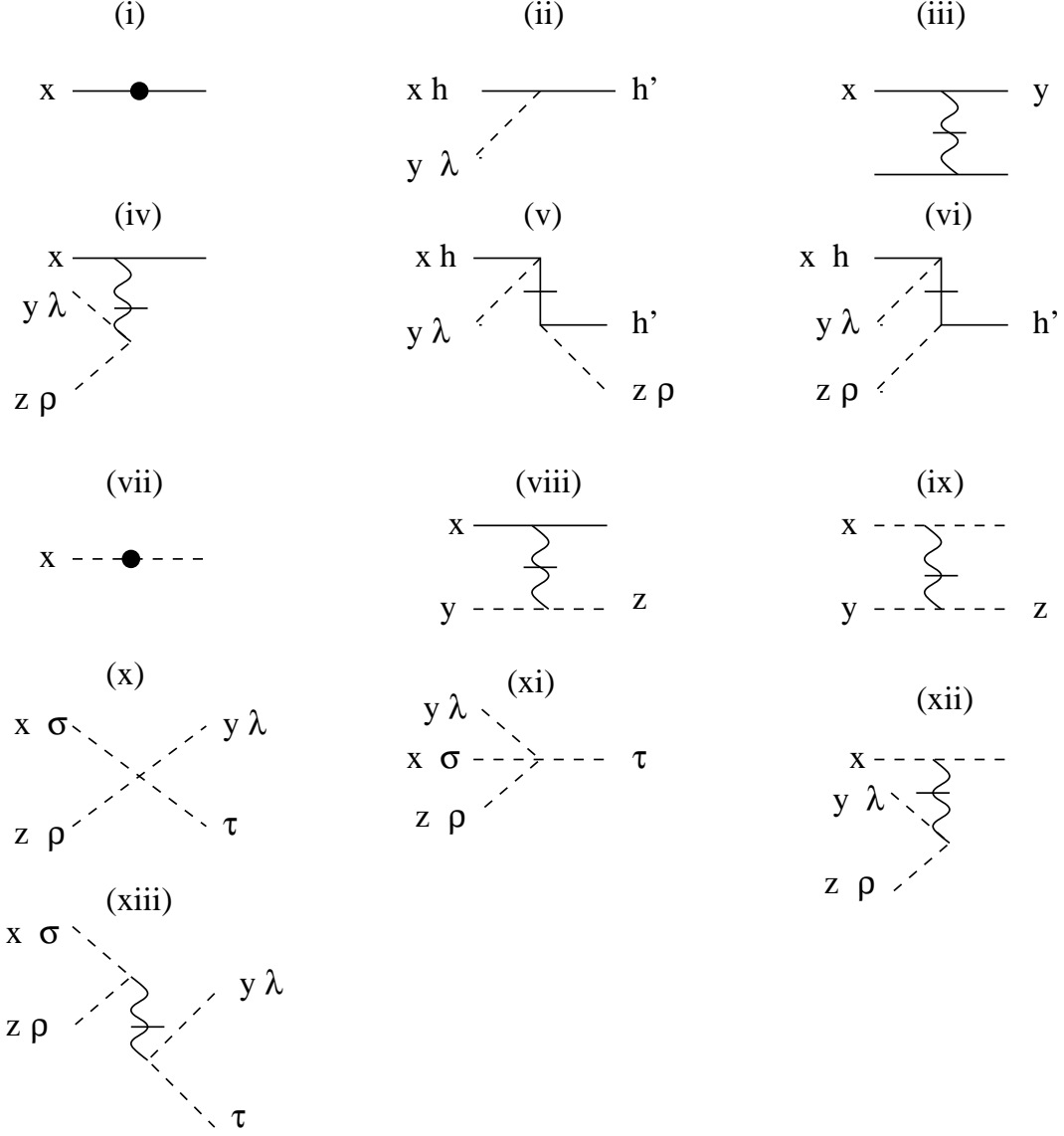


FIG. 5: Planar diagram representation of the elementary interaction vertices following at large N_c . Time x^+ is increasing to the right. Solid lines are quarks, chain lines are link fields. x, y, z represent lightcone momentum fractions, h, h' helicities, $\lambda, \sigma, \rho, \tau \in \{\pm 1, \pm 2\}$ transverse orientation of links. Vertical barred lines are x^+ -instantaneous interactions. Spectator partons in the hadron are not drawn.

TABLE II: Matrix elements of the invariant mass operator $2P^+P^-$ (for zero tranverse momentum) in Fock space; see Fig. 5 for corresponding diagrams of interaction vertices. Momentum conserving delta functions are omitted for clarity. P stands for principal part. $\text{Perp}(\lambda, \rho) = 1$ if $|\lambda| \neq |\rho|$ and 0 otherwise.

$\frac{1}{x} \left(\mu_f^2 + \frac{(\kappa_a^2 + \kappa_s^2) N_c}{\pi} \int_0^x \frac{dy}{y} \right)$	(i)
$\frac{1}{2\sqrt{\pi y}} \left\{ - \left(\frac{1}{x+y} + \frac{1}{x} \right) \mu_f \kappa_s \sqrt{N_c} \delta_{hh'} + \left(\frac{1}{x+y} - \frac{1}{x} \right) \mu_f \kappa_a \sqrt{N_c} \zeta^\lambda_{h'h} \right\}$	(ii)
$\frac{-G^2 N_c}{2\pi} \text{P} \left(\frac{1}{(x-y)^2} \right)$	(iii)
$\frac{-G^2 N_c (y-z)}{4\pi (y+z)^2 \sqrt{yz}} \delta_{-\lambda\rho}$	(iv)
$\frac{N_c}{4\pi (x+y) \sqrt{yz}} \left\{ \kappa_s^2 \delta_{hh'} + \kappa_a^2 (\zeta^\rho \zeta^\lambda)_{h'h} + \kappa_a \kappa_s (\zeta^\rho + \zeta^\lambda)_{h'h} \right\}$	(v)
As (v) with $\rho \rightarrow -\rho$	(vi)
$\frac{m_b^2}{x}$	(vii)
$\frac{-G^2 N_c}{4\pi} \text{P} \left(\frac{y+z}{\sqrt{zy}(z-y)^2} \right)$	(viii)
$\frac{-G^2 N_c}{8\pi} \text{P} \left(\frac{(y+z)(2x+y-z)}{\sqrt{xzy(x+y-z)(z-y)^2}} \right)$	(ix)
$\frac{1}{4\pi \sqrt{xyz(x+z-y)}} \left\{ 2\lambda_1 \delta_{\sigma\lambda} \delta_{\rho\tau} \delta_{-\rho\sigma} + \lambda_2 (\delta_{\sigma\lambda} \delta_{\rho\tau} \delta_{\rho\sigma} + \delta_{-\sigma\rho} \delta_{-\lambda\tau} \delta_{-\sigma\lambda}) \right.$ $\left. + \lambda_4 (\delta_{\sigma\lambda} \delta_{\rho\tau} \text{Perp}(\sigma, \rho) + \delta_{-\sigma\rho} \delta_{-\lambda\tau} \text{Perp}(\sigma, \lambda)) - \beta \delta_{\lambda\rho} \delta_{\sigma\tau} \text{Perp}(\sigma, \rho) \right\}$	(x)
$\frac{1}{4\pi \sqrt{xyz(x+z+y)}} \left\{ 2\lambda_1 \delta_{-\sigma\lambda} \delta_{\lambda\tau} \delta_{\lambda\rho} + \lambda_2 \delta_{\sigma\tau} \delta_{-\lambda\rho} \delta_{ \lambda \sigma } \right.$ $\left. + \lambda_4 (\delta_{-\lambda\sigma} \delta_{\rho\tau} \text{Perp}(\lambda, \rho) + \delta_{-\sigma\rho} \delta_{\lambda\tau} \text{Perp}(\sigma, \lambda)) - \beta \delta_{-\lambda\rho} \delta_{\sigma\tau} \text{Perp}(\sigma, \lambda) \right\}$	(xi)
$\frac{-G^2 N_c}{8\pi} \frac{(y-z)(2x+y+z)}{\sqrt{xzy(x+y+z)(z+y)^2}} \delta_{-\lambda\rho}$	(xii)
$\frac{-G^2 N_c}{8\pi} \frac{(x-z)(2y-x-z)}{\sqrt{xzy(x-y+z)(z+x)^2}} \delta_{-\sigma\rho} \delta_{-\lambda\tau}$	(xiii)

-
- [1] W. A. Bardeen and R. B. Pearson, Phys. Rev. D **14**, 547 (1976).
[2] M. Burkardt and S. Dalley, Prog. Part. Nucl. Phys. **48**, 317 (2002) [arXiv:hep-ph/0112007].
[3] G. 't Hooft, Nucl. Phys. B **75**, 461 (1974).

- [4] F. Antonuccio, S. J. Brodsky, and S. Dalley, Phys. Lett. B **412**, 104 (1997) [arXiv:hep-ph/9705413].
- [5] S. Dalley and B. van de Sande, Phys. Rev. D **56**, 7917 (1997) [arXiv:hep-ph/9704408].
- [6] S. Dalley and T. R. Morris, Int. J. Mod. Phys. A **5**, 3929 (1990).
- [7] S. Dalley and B. van de Sande, Phys. Rev. D **67**, 114507 (2003) [arXiv:hep-ph/0212086].
- [8] S. Dalley and B. van de Sande, Phys. Rev. Lett. **82**, 1088 (1999) [arXiv:hep-th/9810236];
Phys. Rev. D **62**, 014507 (2000) [arXiv:hep-lat/9911035].
- [9] S. Dalley, Phys. Rev. D **64**, 036006 (2001) [arXiv:hep-ph/0101318].
- [10] M. V. Polyakov and C. Weiss, Phys. Rev. D **60**, 114017 (1999) [arXiv:hep-ph/9902451];
I. V. Anikin *et al*, Nucl. Phys. A **678**, 175 (2000) [arXiv:hep-ph/9905332];
A. Mukherjee, I. V. Musatov, H-C. Pauli, and A. V. Radyushkin, Phys. Rev. D **67**,
073014 (2003) [arXiv:hep-ph/0205315];
W. Broniowski and E. Ruiz Arriola, Phys. Lett. B **574**, 57 (2003) [arXiv:hep-ph/0307198];
in *Lightcone Physics: Hadrons and Beyond*, p182 (Durham IPPP, 2003)
[arXiv:hep-ph/0310048];
L. Theussl, S. Noguera and V. Vento, Eur. Phys. J. A **20**, 483 (2004)
[arXiv:nucl-th/0211036];
F. Bissey *et al.*, Phys. Lett. B **587**, 189 (2004) [arXiv:hep-ph/0310184];
M. Praszalowicz and A. Rostworowski, Acta Phys.Polon. B **34**, 2699 (2003)
[arXiv:hep-ph/0302269].
- [11] M. Diehl, Phys. Rept. **388**, 41 (2003) [arXiv:hep-ph/0307382].